RZ-OOK to NRZ-OOK format conversion based on a single fiber Bragg grating

Hui Cao (曹 辉)[1], Xuewen Shu (舒学文)[2*], Javid Atai[3], Qian Dong (董 骞)[1], Jun Zuo (左 军)[1], Guojie Chen (陈国杰)[1], and Yu Yu (余 宇)[2]

[1]*School of Electronics and Information Engineering, Foshan University, Foshan 528000, China*

[2]*Wuhan National Laboratory for Optoelectronics and School of Optoelectronic Science and Engineering, Huazhong University of Science and Technology, Wuhan 430074, China*

[3]*School of Electrical and Information Engineering, The University of Sydney, Sydney, NSW 2006, Australia*

[*]*Corresponding author: xshu@hust.edu.cn*

Received March 24, 2014; accepted June 11, 2014; posted online August 26, 2014

We propose a return-to-zero on-off keying (RZ-OOK) to non-return-to-zero (NRZ) OOK conversion scheme based on a single custom-designed fiber Bragg grating (FBG). The custom-made FBG is designed and synthesized using discrete layer-peeling algorithm. It is shown that such a FBG can replace the combination of interferometer and the cascaded filter that are invariably employed together in the reported schemes for RZ-OOK to NRZ-OOK format conversion. Simulation results show that the input 20-Gb/s RZ-OOK signals with different duty cycles can be converted into NRZ-OOK signals with high Q-factor.

OCIS codes: 060.3735,060.2340, 060.4080.
doi: 10.3788/COL201412.090603.

All-optical format conversion is an important interface technology for future optical transparent networks that will include different formats[1,2]. For instance, with the conversion between return-to-zero (RZ) and non-return-to-zero (NRZ) formats, the optical communication system will be more robust and more flexible for use in different networks such as optical time division multiplexing and wavelength division multiplexing networks[3,4]. The conversion from RZ to NRZ can be realized using various schemes[5–11]. Among the reported schemes, the spectrum-tailoring-based converter is all-passive and very attractive compared with time-domain waveform processing based on active operation device. This is mainly owing to the advantages of the former such as the simplicity of the structure and stable performance[5–11].

Although fiber Bragg grating (FBG) is a versatile optical filter and has been used in some schemes, such as Mach–Zehnder interferometer cascaded narrow-band filter and optical fiber delay interferometer (DI) cascaded narrow-band filter[5–8,11], it only plays a supporting role. In Ref. [12], FBG played a critical role. However, the FBG employed in this scheme is a uniform one, wherein the sidelobes of amplitude transfer function seriously affect the performance of format conversion. To reduce the influence of the FBG sidelobes, they have to choose either a weak FBG (the maximum reflectivity of 21%) or a strong FBG with an additional Gaussian optical band-pass filter with narrow bandwidth[12], which means high insertion loss is inevitable in both cases. In other words, the filtering capability of FBG is not fully utilized in the reported schemes since a variety of filter function can be achieved by a properly designed FBG. In this work, we propose and simulate one customized FBG-based single filter to substitute interferometer and the cascaded filter that are invariably employed together in the reported schemes to fulfill RZ on-off keying (OOK) to NRZ-OOK format conversion. The spectral response of this FBG is customized according to the optical spectral response of the DI cascaded narrow-band filter. Simulation results show that the designed FBG is capable of converting 20-Gb/s RZ-OOK signals with different duty cycles to NRZ-OOK signals.

As is shown in Fig. 1, the principle of operation of the single FBG-based format conversion scheme is similar to that of DI cascaded filter scheme. In the DI cascaded filter scheme, the peak transmission wavelengths of the DI are adjusted to aim at the carrier of the RZ-OOK signal and the even sidebands. On the other hand, the notches are aimed at the odd sidebands to suppress them. The cascaded filter is designed to filter the residual even sidebands to finally complete the format conversion. To sum up, two steps as well as two devices are needed to fulfill the spectral tailoring process. However, in our FBG-based scheme only one step is needed to tailor the RZ-OOK spectra into the NRZ-OOK spectra. It should be noted that the FBG in our scheme is a single channel one. In our FBG-based scheme, the peak wavelength of the spectral response is designed to aim at the center of the RZ-OOK signal, while the bandwidth is customized to pass the main lobe but suppress all the sidebands.

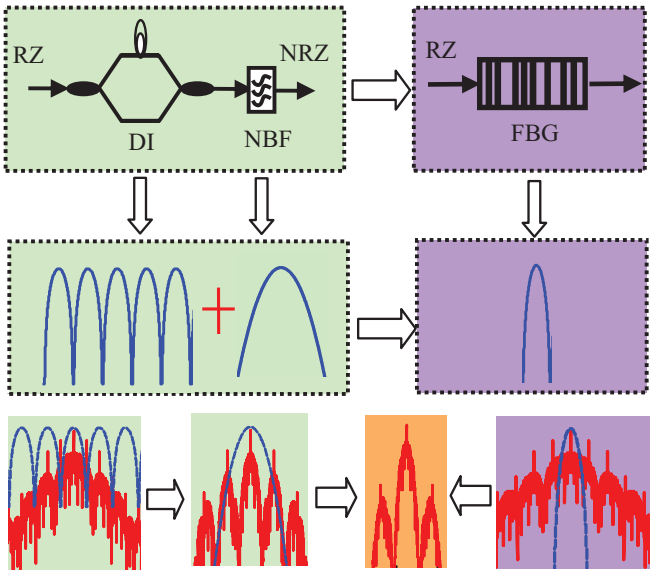

Fig. 1. Principle comparison of single FBG scheme and DI cascaded filter scheme. NBF, narrow-band filter.

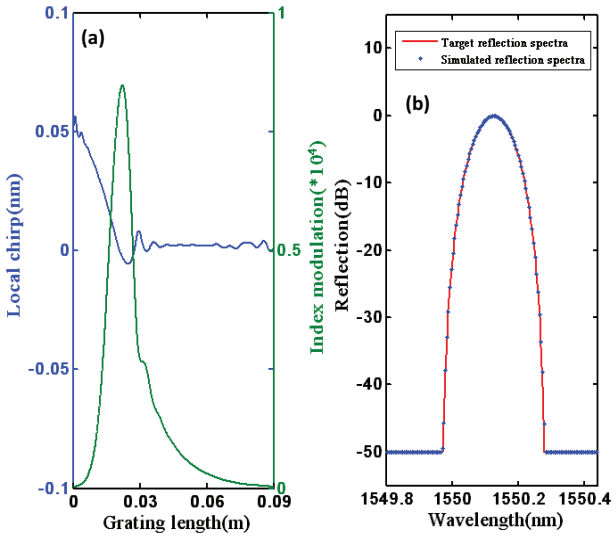

Fig. 2. Structure and optical response of the synthesized FBG filter: (a) synthesized index modulation (green line) and local chirp (blue line) and (b) simulated reflection spectra (dotted blue line) and target reflection spectra (solid red line).

Another important issue is the actual profile of the spectra response. One way to determine the profile is to use the overall spectral response of DI cascaded filter scheme. That is, one can calculate the FBG spectral response by multiplying the transmission spectra of DI by that of the narrow-band filter. For instance, in the case of a DI with 40 GHz free spectral range (FSR) that is cascaded with a filter with 3-dB bandwidth of 0.3 nm for 20-Gb/s RZ-OOK to NRZ-OOK format conversion[5–7], the FBG spectral response can be expressed as

$$R(\lambda)=\frac{1}{2}\left(1+\cos\left(2\pi c\left(\frac{1}{\lambda}-\frac{1}{\lambda_c}\right)\times\Delta t\right)\right)\times\exp\left(-\ln(2)\times\left(\frac{2(\lambda-\lambda_c)}{0.3}\right)^2\right), \quad (1)$$

where c is the velocity of light in vacuum, $\Delta t = 0.025$ ns for 40 GHz FSR, and λ_c is the carrier wavelength of RZ signal.

Given spectral response in Eq. (1), one can utilize the layer-peeling algorithm to synthesize the grating[13]. The synthesized grating structure with the grating length of 9 cm is shown in Fig. 2(a). It is worth noting that the maximum refractive index modulation and maximum local chirp are 0.000085 and 0.06 nm, respectively. These values are well within the practically realizable range. Furthermore, Fig. 2(b) displays the results of the simulated reflection spectra of the designed FBG. As shown, the simulated reflection spectra (dotted blue line) are in excellent agreement with the target reflection spectra (solid red line). This indicates that the designed FBG complies fully with the requirements of Eq. (1).

In order to investigate the capabilities of the designed FBG, we have performed simulations of 20-Gb/s RZ-OOK to NRZ-OOK conversion with pseudo-random binary sequence (PRBS) of length 2^{31}-1 bits. All the simulations are carried out with Matlab according to the methods described in Refs. [5–7]. In the simulations, two small duty cycles (20% and 33%) as well as two large duty cycles (50% and 67%) are chosen to adequately investigate the performance of our scheme. Note that we only consider the duty cycles rather than the polarity of electric field waveforms, so the unipolar electric field waveforms are necessary for all four duty cycles in simulation. Figures 3(a)–(c) show the waveforms, spectra, and eye diagrams of the RZ-OOK signals, respectively, and Figs. 3(d)–(f) present the corresponding profiles of the NRZ-OOK signals. Comparing Figs. 3(a) and (d), one can see that the RZ-OOK pulses have been broadened to NRZ-OOK pulses. This is due to the FBG filtering as illustrated in Figs. 3(b) and (e). From this point of view, such a FBG can be employed to convert RZ-OOK signals with different duty cycles to NRZ-OOK signals, in an all-optical and all-passive manner.

It should be noted that although the eye diagrams of the output NRZ-OOK signal are clean and open in the case of small duty cycles, such as 20% and 33%, the Q-factors decrease with the increase in the duty cycle. For example, as shown in Fig. 3(d), in the cases of 67% and 50% duty cycles, a single "1" bit has lower power than the several consecutive "1" bits. This can be attributed to the high-frequency components being excessively suppressed in the cases of larger duty cycles, whereas in the smaller duty cycle cases this excessive suppression is mitigated. As is shown in Fig. 3(b), the smaller the duty cycle, the flatter is the spectra of

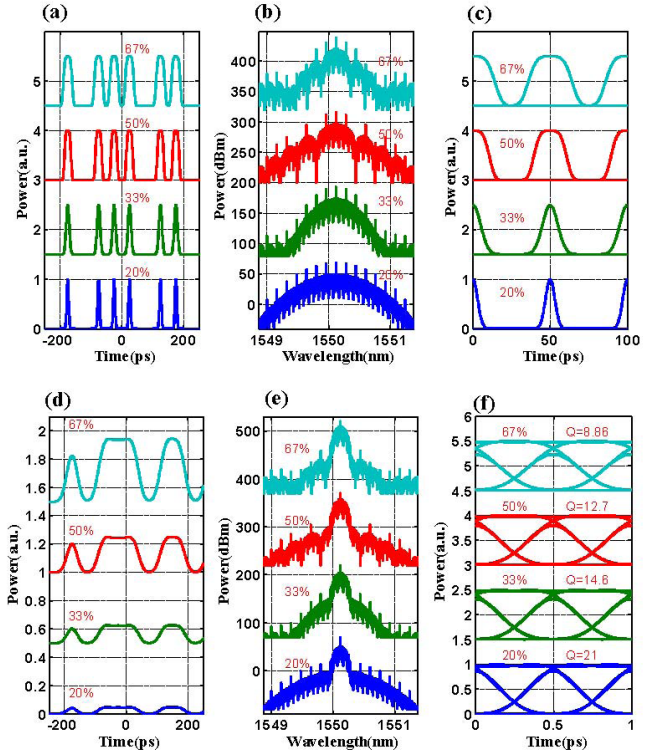

Fig. 3. (a) Simulated waveforms, (b) spectra, and (c) eye diagrams of the input RZ-OOK signals at 20-Gb/s and (d)–(f) the corresponding output NRZ-OOK signals, with four different duty cycles (20%, 33%, 50%, and 67%). Note that all the curves in the same sub-figure have been offset for clarity and eye diagrams in (f) have been normalized for clear comparison.

RZ-OOK signals. In other words, in the main lobe, the proportions of the high-frequency components increase as duty cycle decreases. This is helpful to mitigate the excessive high-frequency suppression. These problems can be avoided by designing the FBG spectral response using other methods, such as theoretical deduction and mathematical optimization techniques. We are currently investigating these approaches. Alternatively, one can detune the central wavelength or broaden the bandwidth of the designed FBG to partly mitigate the excessive high-frequency suppression, as discussed below.

To further investigate the performance of this scheme as well as fabrication tolerances, we simulate two kinds of deviations from the ideal model. In the first case, the central wavelength of FBG reflection band is detuned from the carrier wavelength. Figure 4 shows the Q-factor as a function of the filter wavelength detuning. It is interesting to note that in Fig. 4 each Q-factor curve has a concave shape around the center (roughly within ±0.02 nm depend on duty cycle). This means one can possibly tune the FBG center wavelength to obtain a higher Q-factor. The reason that a moderate filter detuning (roughly within ±0.02 nm), either red-shift or blue-shift, can enhance rather than degrade the performance is that the moderate filter detuning benefits mitigating excessive suppression of the high-frequency components

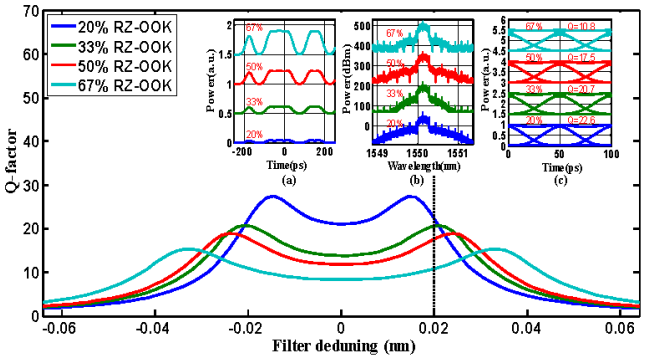

Fig. 4. Q-factor as a function of the filter detuning for four different duty cycles (20%, 33%, 50%, and 67%). Insets are the (a) simulated waveforms, (b) spectra, and (c) eye diagrams of the output NRZ-OOK signals with the filter detuning of 0.02 nm, respectively.

in the filtering, as shown in the insets. An over-detuning can obviously degrade the performance due to the fact that it can result in the carrier being over filtered and therefore seriously affect format conversions.

In the second case, we consider the deviations of FBG bandwidth from the originally designed one (~0.32 nm). We simulate the bandwidth deviation values in the range from − 0.08 to + 0.08 nm to consider both narrowing and broadening cases. Figure 5 shows the variation of the Q-factor as a function of bandwidth deviation value for four different duty cycles. It is interesting to see in Fig. 5 that the bandwidth broadening, in a certain range, can increase the value of the Q-factor while the bandwidth narrowing can only result in the monotonic decreasing of the Q-factor. It is also noted from Fig. 5 that the Q-factor can be optimized at slightly different bandwidths for different duty cycles. The inset in Fig. 5 shows the eye diagrams for four different duty cycles when the FBG bandwidth is broadened with 0.02 nm. Compared with Fig. 3(f), one can find that the performance shown in the inset of Fig. 5 is better than that of the original bandwidth. Figure 5 also demonstrates that the best conversion performance

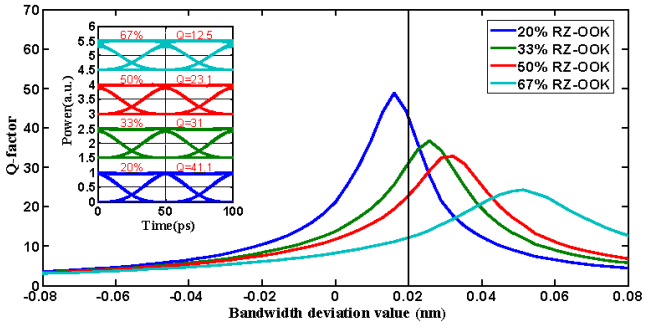

Fig. 5. Q-factor as a function of bandwidth deviation value for four different duty cycles (20%, 33%, 50%, and 67%). Inset shows the simulated eye diagrams of the output NRZ-OOK signals with bandwidth deviation value of 0.02 nm.

can be achieved at slightly different bandwidth for different duty cycles.

In conclusion, we propose and simulate a single FBG-based RZ-OOK to NRZ-OOK format conversion. Simulation results show that the designed FBG can convert 20-Gb/s RZ-OOK signal with different duty cycles to NRZ-OOK signal with high Q-factor. Detuning the central wavelength and broadening the bandwidth of the designed FBG in a certain range are two alternative methods to partly mitigate the excessive high-frequency suppression and to further increase the Q-factor of the output NRZ-OOK signals. The proposed single FBG scheme does not require any active components. It is free from any interferometric instability and introduces no additional amplified spontaneous emission noise.

This work was supported by the National Natural Science Foundation of China (No. 61178030), the Natural Science Foundation of Guangdong Province, China (No. S201101000122), the Fundamental Research Funds for the Central Universities, China (No. HUST2013TS047), and the Fundamental Research Funds of Foshan University.

References

1. Y. Zhan, M. Zhang, M. Liu, L. Liu, and X. Chen, Chin. Opt. Lett. **11,** 030604 (2013).
2. Y. Zhang, L. Yi, T. Zhang, Z. Li, and W. Hu, Chin. Opt. Lett. **11,** 100601 (2013).
3. P. J. Winzer and R. J. Essiambre, Proc. IEEE **94,** 952 (2006).
4. W. Yu, C. Lou, X. Zhao, and D. Lu, Chin. Opt. Lett. **8,** 859 (2010).
5. Y. Yu, X. Zhang, and D. Huang, in *Proceedings of 2006 Optics Valley of China International Symposium on Optoelectronics* 47 (2006).
6. Y. Yu, Z. Xinliang, D. Huang, L. Lijun, and F. Wei, IEEE Photon. Technol. Lett. **19,** 1027 (2007).
7. Y. Yu, X. Zhang, and D. Huang, Opt. Commun. **284,** 129 (2011).
8. F. Wang, E. Xu, Y. Yu, and Y. Zhang, Proc. SPIE **8308,** 83080E (2011).
9. S. G. Park, L. Spiekman, M. Eiselt, and J. Weisenfeld, IEEE Photon. Technol. Lett. **12,** 233 (2000).
10. A. L. Yi, L. S. Yan, B. Luo, W. Pan, J. Ye, Z. Y. Chen, and J. Lee, Opt. Express **20,** 9890 (2012).
11. P. Groumas, V. Katopodis, C. Kouloumentas, M. Bougioukos, and H. Avramopoulos, IEEE Photon. Technol. Lett. **24,** 179 (2012).
12. O. Ozolins, V. Bobrovs, and G. Ivanovs, in *Proceedings of 55th International Symposium ELMAR 2013* 121 (2013).
13. H. Cao, J. Atai, X. Shu, and G. Chen, Opt. Express **20,** 12095 (2012).